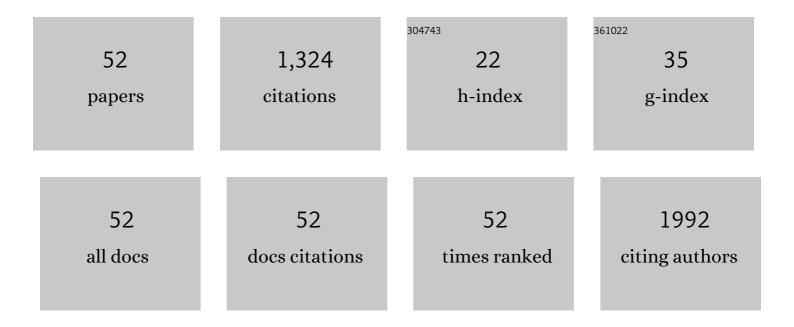
Bram Trachet

List of Publications by Year in descending order

Source: https://exaly.com/author-pdf/9509754/publications.pdf Version: 2024-02-01



#	Article	IF	CITATIONS
1	Outflow Through Aortic Side Branches Drives False Lumen Patency in Type B Aortic Dissection. Frontiers in Cardiovascular Medicine, 2021, 8, 710603.	2.4	6
2	Co-localization of microstructural damage and excessive mechanical strain at aortic branches in angiotensin-II-infused mice. Biomechanics and Modeling in Mechanobiology, 2020, 19, 81-97.	2.8	11
3	Noninvasive Cardiac Output and Central Systolic Pressure From Cuff-Pressure and Pulse Wave Velocity. IEEE Journal of Biomedical and Health Informatics, 2020, 24, 1968-1981.	6.3	23
4	Early Morphofunctional Changes in AngII-Infused Mice Contribute to Regional Onset of Aortic Aneurysm and Dissection. Journal of Vascular Research, 2020, 57, 367-375.	1.4	4
5	Synchrotron-based visualization and segmentation of elastic lamellae in the mouse carotid artery during quasi-static pressure inflation. Journal of the Royal Society Interface, 2019, 16, 20190179.	3.4	7
6	On the importance of the nonuniform aortic stiffening in the hemodynamics of physiological aging. American Journal of Physiology - Heart and Circulatory Physiology, 2019, 317, H1125-H1133.	3.2	10
7	Propagation-based phase-contrast synchrotron imaging of aortic dissection in mice: from individual elastic lamella to 3D analysis. Scientific Reports, 2018, 8, 2223.	3.3	23
8	Should We Ignore What We Cannot Measure? How Non-Uniform Stretch, Non-Uniform Wall Thickness and Minor Side Branches Affect Computational Aortic Biomechanics in Mice. Annals of Biomedical Engineering, 2018, 46, 159-170.	2.5	9
9	Synchrotron-based phase contrast imaging of cardiovascular tissue in mice—grating interferometry or phase propagation?. Biomedical Physics and Engineering Express, 2018, 5, 015010.	1.2	3
10	TGFβ (Transforming Growth Factor-β) Blockade Induces a Human-Like Disease in a Nondissecting Mouse Model of Abdominal Aortic Aneurysm. Arteriosclerosis, Thrombosis, and Vascular Biology, 2017, 37, 2171-2181.	2.4	64
11	Angiotensin II infusion into ApoE-/- mice: a model for aortic dissection rather than abdominal aortic aneurysm?. Cardiovascular Research, 2017, 113, 1230-1242.	3.8	78
12	The influence of anesthesia and fluid–structure interaction on simulated shear stress patterns in the carotid bifurcation of mice. Journal of Biomechanics, 2016, 49, 2741-2747.	2.1	22
13	Pitfalls of Doppler Measurements for Arterial Blood Flow Quantification in Small Animal Research: A Study Based on Virtual Ultrasound Imaging. Ultrasound in Medicine and Biology, 2016, 42, 1399-1411.	1.5	3
14	Ascending Aortic Aneurysm in Angiotensin II–Infused Mice. Arteriosclerosis, Thrombosis, and Vascular Biology, 2016, 36, 673-681.	2.4	65
15	Shear Stress Metrics and Their Relation to Atherosclerosis: An In Vivo Follow-up Study in Atherosclerotic Mice. Annals of Biomedical Engineering, 2016, 44, 2327-2338.	2.5	21
16	Assessment of shear stress related parameters in the carotid bifurcation using mouse-specific FSI simulations. Journal of Biomechanics, 2016, 49, 2135-2142.	2.1	26
17	A 1D model of the arterial circulation in mice. ALTEX: Alternatives To Animal Experimentation, 2016, 33, 13-28.	1.5	17
18	Vulnerable Plaque Detection and Quantification with Gold Particle–Enhanced Computed Tomography in Atherosclerotic Mouse Models. Molecular Imaging, 2015, 14, 7290.2015.00009.	1.4	12

BRAM TRACHET

#	Article	IF	CITATIONS
19	Performance Comparison of Ultrasound-Based Methods to Assess Aortic Diameter and Stiffness in Normal and Aneurysmal Mice. PLoS ONE, 2015, 10, e0129007.	2.5	22
20	Editorial (Thematic Issue: Novel Insights on Aortic Aneurysm). Current Pharmaceutical Design, 2015, 21, 3993-3995.	1.9	1
21	Incidence, severity, mortality, and confounding factors for dissecting AAA detection in angiotensin II-infused mice: a meta-analysis. Cardiovascular Research, 2015, 108, 159-170.	3.8	31
22	An Animal-Specific FSI Model of the Abdominal Aorta in Anesthetized Mice. Annals of Biomedical Engineering, 2015, 43, 1298-1309.	2.5	28
23	Intrinsic cardiomyopathy in Marfan syndrome: results from in-vivo and ex-vivo studies of the Fbn1C1039G/+ model and longitudinal findings in humans. Pediatric Research, 2015, 78, 256-263.	2.3	45
24	Dissecting abdominal aortic aneurysm in Ang II-infused mice: suprarenal branch ruptures and apparent luminal dilatation. Cardiovascular Research, 2015, 105, 213-222.	3.8	59
25	Dissecting abdominal aortic aneurysm in Angiotensin II-infused mice: the importance of imaging. Current Pharmaceutical Design, 2015, 21, 4049-4060.	1.9	8
26	Emerging Pharmacological Treatments to Prevent Abdominal Aortic Aneurysm Growth and Rupture. Current Pharmaceutical Design, 2015, 21, 4000-4006.	1.9	12
27	Absence of Cardiovascular Manifestations in a Haploinsufficient Tgfbr1 Mouse Model. PLoS ONE, 2014, 9, e89749.	2.5	9
28	Longitudinal follow-up of ascending versus abdominal aortic aneurysm formation in angiotensin II-infused ApoEâ~'/â~' mice. Artery Research, 2014, 8, 16.	0.6	4
29	A multi-angle plane wave imaging approach for high frequency 2D flow visualization in small animals: Simulation study in the murine arterial system. , 2014, , .		1
30	Haemodynamic impact of stent–vessel (mal)apposition following carotid artery stenting: mind the gaps!. Computer Methods in Biomechanics and Biomedical Engineering, 2013, 16, 648-659.	1.6	27
31	A computational method to assess the in vivo stresses and unloaded configuration of patient-specific blood vessels. Journal of Computational and Applied Mathematics, 2013, 246, 10-17.	2.0	107
32	Characterization of Cardiovascular Involvement in Pseudoxanthoma Elasticum Families. Arteriosclerosis, Thrombosis, and Vascular Biology, 2013, 33, 2646-2652.	2.4	62
33	Role of the renin–angiotensin system on abdominal aortic aneurysms. European Journal of Clinical Investigation, 2013, 43, 1328-1338.	3.4	34
34	A Computational Study of the Hemodynamic Impact of Open- Versus Closed-Cell Stent Design in Carotid Artery Stenting. Artificial Organs, 2013, 37, E96-E106.	1.9	15
35	Inverse modelling of image-based patient-specific blood vessels: zero-pressure geometry and <i>in vivo</i> stress incorporation. ESAIM: Mathematical Modelling and Numerical Analysis, 2013, 47, 1059-1075.	1.9	7
36	CFD Challenge: Solutions Using the Commercial Finite Volume Solver, Fluent, and a pyFormex-Generated Full Hexahedral Mesh. , 2012, , .		0

BRAM TRACHET

#	Article	IF	CITATIONS
37	The Ghent Marfan Trial — A randomized, double-blind placebo controlled trial with losartan in Marfan patients treated with β-blockers. International Journal of Cardiology, 2012, 157, 354-358.	1.7	59
38	Effect of the degree of LAD stenosis on "competitive flow―and flow field characteristics in LIMA-to-LAD bypass surgery. Medical and Biological Engineering and Computing, 2012, 50, 839-849.	2.8	22
39	Validation of the Arteriograph working principle: questions still remain. Journal of Hypertension, 2011, 29, 619.	0.5	9
40	Validation of the arteriograph working principle. Journal of Hypertension, 2011, 29, 1662-1663.	0.5	3
41	Replacing Vascular Corrosion Casting by In Vivo Micro-CT Imaging for Building 3D Cardiovascular Models in Mice. Molecular Imaging and Biology, 2011, 13, 78-86.	2.6	40
42	An Integrated Framework to Quantitatively Link Mouse-Specific Hemodynamics to Aneurysm Formation in Angiotensin II-infused ApoE â^'/â^' mice. Annals of Biomedical Engineering, 2011, 39, 2430-2444.	2,5	43
43	The Impact of Simplified Boundary Conditions and Aortic Arch Inclusion on CFD Simulations in the Mouse Aorta: A Comparison With Mouse-specific Reference Data. Journal of Biomechanical Engineering, 2011, 133, 121006.	1.3	27
44	Structural Simulation of a Mouse-Specific Abdominal Aorta. , 2011, , .		0
45	Numerical Validation of a New Method to Assess Aortic Pulse Wave Velocity from a Single Recording of a Brachial Artery Waveform with an Occluding Cuff. Annals of Biomedical Engineering, 2010, 38, 876-888.	2.5	81
46	Validation of the murine aortic arch as a model to study human vascular diseases. Journal of Anatomy, 2010, 216, 563-571.	1.5	29
47	Vascular corrosion casting: analyzing wall shear stress in the portal vein and vascular abnormalities in portal hypertensive and cirrhotic rodents. Laboratory Investigation, 2010, 90, 1558-1572.	3.7	32
48	Resolving in-vivo flow fields in the systemic circulation of the mouse through combined ultrasound imaging and computational fluid dynamics. , 2010, , .		0
49	The influence of aortic dimensions on calculated wall shear stress in the mouse aortic arch. Computer Methods in Biomechanics and Biomedical Engineering, 2009, 12, 491-499.	1.6	23
50	Limitations and pitfalls of non-invasive measurement of arterial pressure wave reflections and pulse wave velocity. Artery Research, 2009, 3, 79.	0.6	79
51	Wall shear stress in the mouse aortic arch : Does size matter?. IFMBE Proceedings, 2009, , 1994-1998.	0.3	1
52	Patient-Specific Modelling of Aortic Arch Wall Shear Stress Patterns in Patients With Marfan Syndrome. , 2009, , .		0